Water Air Soil Pollut (2020) 231: 508
https://doi.org/10.1007/s11270-020-04884-5

Physicochemical Characterization of Airborne Particulate Matter in Medellín, Colombia, and its Use in an In Silico Study of Ventricular Action Potential

Camilo Zapata-Hernandez · Geraldine Durango-Giraldo · Catalina Tobón · Robison Buitrago-Sierra

Received: 16 June 2020 / Accepted: 22 September 2020 / Published online: 29 September 2020

Abstract Particulate matter (PM) is a complex mixture of particles that changes over time and from place to place; however, most PM is caused by the fuel combustion of motor vehicles and industry. PM is associated with acute and chronic illnesses, such as pulmonary and cardiovascular diseases. Medellín is one of the most polluted cities in Latin America. Therefore, the physicochemical characterization of its PM is necessary to understand its composition and effect on human health. In this study, PM was characterized by scanning electron microscopy (SEM), energy dispersive x-ray spectroscopy (EDS) analysis, Fourier infrared spectroscopy (FTIR), inductivity-coupled plasma optical emission spectrometry (ICP-OES), and thermogravimetric analysis (TGA) in order to evaluate its morphology and chemical composition. The SEM of the PM exhibited primary particles and agglomerates. The size of the particles ranged between 0.056 and 4.5 μm. The EDS revealed elements such as carbon, silicon, calcium, lead, and iron. Furthermore, carbon monoxide, carbon dioxide, and carbonyl and aliphatic functional groups were observed by means of FTIR. Additionally, weight losses associated with volatile matter and elemental carbon were identified in the TGA analysis. The TGA and FTIR confirmed the presence of fuel and lubricant traces. Subsequently, lead was selected among the most common components in the PM in order to conduct an in silico study into its effect on ventricular activity. Lead showed a pro-arrhythmic effect by shortening the duration of the action potential under normal electrophysiological conditions, which could be associated with cardiovascular diseases.

Keywords Air pollution · Particulate matter composition · Computer simulation · Heart diseases

C. Zapata-Hernandez · G. Durango-Giraldo · R. Buitrago-Sierra (✉)
MATyER, Facultad de Ingeniería, Instituto Tecnológico Metropolitano, Cll. 54 A, #30-01 Medellín, Colombia
e-mail: robinsonbuitrago@itm.edu.co

C. Tobón
MATBIOM, Facultad de Ciencias Básicas, Universidad de Medellín, Cra. 87, #30-65 Medellín, Colombia

1 Introduction

Particulate matter (PM) is a mixture of solid and liquid particles of inorganic and organic substances that are commonly found suspended in the air (Perrino et al. 2015). PM is commonly classified into coarse, fine, and ultrafine particles depending on its aerodynamic diameter. Coarse particles have an aerodynamic diameter between 2.5 and 10 μm (PM_{10}); fine particles, equal to or less than 2.5 μm ($PM_{2.5}$); and ultrafine particles, less than 0.1 μm ($PM_{0.1}$) (Mirowsky et al. 2014; Huang et al. 2017; U.S. EPA. 2018). The particle size of PM is directly related to its potential harmful effects on human health. Coarse PM can penetrate and lodge deep inside the lungs; however, it is not as harmful to human health as $PM_{2.5}$. Fine PM can cross the pulmonary barrier and enter the blood system with adverse health effects (Di Novi 2013; Xing et al. 2016). Other problems caused by

PM include environmental issues such as air acidity (Wu and Zhang 2018), low visibility (Wang et al. 2018), and material damage (Al-Thani et al. 2018).

PM sources can be either human (anthropogenic) or natural (non-anthropogenic). Anthropogenic sources include (diesel and petrol) combustion engines, solid fuels (heavy oil and coal), and the manufacture of cement, ceramics, and bricks, among others. Accordingly, the chemical characteristics of PM change from place to place. Nevertheless, its most common chemical elements include magnesium, sodium, potassium, calcium, copper, lead, and nickel, as well as other compounds such as aromatic hydrocarbons and elemental and organic carbon (Dickerson et al. 2016; Moreira-Lopez et al. 2016; Müller et al. 2017).

The World Health Organization (WHO) has estimated that fine PM causes around 4.6 million premature deaths per year worldwide (World Health Organization 2019). People living in low- and middle-income countries disproportionately experience the burden of air pollution. Numerous epidemiological and clinical studies indicate that PM in air pollution is strongly associated with higher rates of cardiovascular diseases, such as arrhythmias, myocardial infarction, ischemic stroke, vascular dysfunction, hypertension, and atherosclerosis (Di Novi 2013; Chin 2015). Bañeras et al. (2018) found that the daily rate of hospital admissions for ST segment elevation myocardial infarction (STEMI) is associated with increases in concentrations of $PM_{2.5}$, PM_{10}, lead, and NO_2 in the air. In turn, Xia et al. (2018) reported that long-term exposures to PM_{10} are positively associated with subclinical atherosclerosis in middle-aged adults. Therefore, PM size and chemical composition are important to determine the source and the health risk that particulate matter represents for exposed individuals (Davy et al. 2012).

Elements such as calcium (Ca), silicon (Si), iron (Fe), titanium (Ti), and aluminum (Al) have been detected at PM sampling sites in urban as well as sub-urban areas (Bozkurt et al. 2018; Genga et al. 2018). In general, Si, Al, Ca, and Ti are the most common elements in the Earth's crust, products of soil dust, and quarry exploitation (Kholdebarin et al. 2015). However, heavy metals such as chromium (Cr), arsenic (As), cadmium (Cd), lead (Pb), and mercury (Hg) are also present in PM, mostly due to anthropogenic activities (Vimercati et al. 2017; Esposito et al. 2019). Lead is one of the most harmful heavy metals for human health (Wani et al. 2015; Lu et al. 2019). Menke et al. (2006) measured the blood lead level (BLL) of 13,946 individuals in the USA, recruited between 1988 and 1994, for more than 12 years. They observed an association between BLL and myocardial infarction and stroke mortality. This association was evident at levels ≥2 μm/dL. Moreover, Lustbeg and Silbergeld (2015) found that individuals with a BLL from 20 to 29 μm/dL experienced increased circulatory and cardiovascular mortality. Additionally, lead is associated with an increase in blood pressure, heart rate, and heart rate variability (Lim et al. 2017).

The physicochemical features of PM are directly related to its emission source; as a result, PM produced by diesel vehicles, gasoline vehicles, and natural emissions differs significantly. In that sense, the PM in each region in the world also exhibits specific features associated with the type of emission sources of its particles. Therefore, the local characterization of PM is of great importance to understand its effects depending on the particularities of the region. Several studies around the world have examined the correlation between (1) particle size and chemical composition of PM and (2) health risks. Nevertheless, the characterization of this type of particulate matter has not been widely explored, which makes correlating its properties with real observed harmful effects more difficult. Specifically, real particle size should be further investigated because it is one of the most important characteristics of this material, and most of the reports are just based in the filters weight at the monitoring stations, assuming the size of all the collected material. Some alternatives to fill this gap are techniques such as scanning electron microscopy (SEM), which can be used to reliably evaluate the morphology and particle size distribution of PM (Babick et al. 2016). In addition, in the conventional extractive methods employed in the literature, fibers are removed from the filters without any further separation from the PM or quantifying said material in the analysis (De Kok et al. 2005; Škarek et al. 2007).

Medellín is the second largest city in Colombia, with a population of about 2.5 million inhabitants, and its geographical conditions make air pollution worse because the mountain ranges that surround the city cause pollutants to remain longer in the atmosphere (Gomez et al. 2011). Several reports between 2003 and 2015 have shown that, in most of the monitoring stations in said city, the PM_{10} levels exceeded WHO limits in countless occasions. Arias-Valencia et al. (2010) revealed that Medellín experiences an epidemic of mortality due to diseases associated with air pollution; there

are about 3000 deaths per year for that reason, out of which 1500 are related to toxic components in the air. Between 2012 and 2016, $PM_{2.5}$ concentrations exceeded WHO recommendations, and, even worse, they show no sign of decreasing (López et al. 2017).

However, to the best of the authors' knowledge, the physicochemical composition of the PM obtained in Medellín has not been studied in detail so far. In this paper, PM collected in a monitoring station in Medellín is physicochemically and morphologically characterized in depth, and the results are used in an in silico study to evaluate its effect on ventricular action potential.

2 Methods

2.1 Sample Collection

Particulate matter was collected at a certified monitoring station inside the premises of the University of Medellín, Colombia (6°13'N,75°36'O). The University is located southwest of the city, which is considered an urban area. In addition, the sampling point is near a quarry, and the sampling equipment was located on the roof of a building. The particulate matter was collected for 24 h using a quartz microfiber filter (Whatman). The PM was sampled every 4 days between October and November in 2018 using a PM10 Size Selective Sampling Inlet (RFPS 1287–063) provided by Staplex. The volumetric flow was adjusted between 1.038 m^3/min and 1.258 m^3/min, as per Method IO-2.1 established by the US EPA (U.S. EPA. 1999). After the sampling period, the filter was desiccated for 24 h in a desiccator containing silica gel (U.S. EPA. 2016).

2.2 Particulate Matter Extraction

The particulate matter captured during the sampling was extracted from the filters by the Soxhlet method, which is commonly employed for the extraction of particulate matter (Dallarosa et al. 2005; Cavanagh et al. 2009; Masih et al. 2010). The filters were cut into fragments and placed in Soxhlet equipment. The extraction process lasted 24 h at 110 °C. A mixture of deionized water (< 18 MΩ·m) and acetone (Chemi, purity >99.5%) in a 1:2 ratio was used in order to extract polar and no polar components from the filter (Obot et al. 2002; Roper et al. 2015). Afterward, the extract was concentrated using a rotary evaporator and dried at 80 °C in an oven overnight.

2.3 Physicochemical Characterization

The volatile fraction and elemental carbon in the particulate matter were characterized by thermogravimetric analysis (TGA) using a TA Instruments SDT-Q600 Simultaneous TGA/DSC with a heating program in a nitrogen atmosphere, initially, and a ramp of 3 °C per minute up to 450 °C. Subsequently, the program was changed to an air atmosphere and a ramp of 5 °C per minute up to 500 °C. Finally, an isothermal process was conducted for 70 min (Mustafi et al. 2010). Functional groups in the PM were analyzed by infrared spectroscopy with an IRTracer-100 (FTIR) spectrophotometer with wavelengths between 500 and 4000 cm^{-1} by the attenuated total reflection (ATR) method. The size and shape of the PM were determined using a JEOL JSM-7100F (FE-SEM) scanning electron microscope with a voltage of 15 kV and a working distance between 4 and 10 mm. The open-source software Image J was used to measure the diameter of more than 550 particles in approximately 100 micrographs. The measurement of the particles size with the software can be divided into two steps, in the first part the calibration of the SEM image in order to correlate the image dimensions in pixel to physical dimensions is performed. In the second part, the particles are measured by using the tools of the software, since some particles are not totally spherical, the Feret's diameter is employed to calculate their size (Mazzoli and Favoni 2012). Likewise, the raw filters were also studied by FE-SEM before being used and after particulate matter collection. The chemical composition of the PM was obtained by energy dispersive spectrometry (EDS) using an X-MaxN SDD detector (available from Oxford Instruments) attached to a scanning electron microscope with a voltage of 20 kV; for that purpose, more than 20 analyses were performed. In addition, heavy metals were determined and quantified using a Thermo Fisher Scientific™ iCAP™ 7000 Series ICP-OES (Inductivity Coupled Plasma Optical Emission Spectrometer) as per the 23rd edition of APHA Standard Methods 3120 A and 3120 B. The PM characterization was performed using all the material extracted from all the filters after the washing process.

2.4 Model of the Effects of Lead on Ventricular Action Potential

Based on a study into myocytes, which showed that lead (Pb) affects the cardiac electrical activity by blocking the L-type calcium channel (I_{CaL}) (Bernal et al. 1997), we used Hill's equation to fit the concentration-response relationship of the I_{CaL} current block caused by lead. Therefore, the fraction of block (b_{Pb}) is described in Eq. (1):

$$b_{Pb} = \frac{1}{\left[1 + \frac{IC_{50}}{D}\right]^{h}} \quad (1)$$

where IC_{50} is the half maximal inhibitory concentration, which is equal to 152 nM, a value found by Bernal et al. (1997) in ventricular myocytes; D is the lead concentration; and h is the Hill coefficient, where a value of 1 indicates a completely independent binding. The factor ($1–b_{Pb}$) was included in the I_{CaL} equation of the O'Hara-Rudy-CiPA ventricular single-cell model (Dutta et al. 2017). Such model was used to simulate the human endocardial ventricular action potential. The publicly available software CellML OpenCOR® was used to simulate a train of 1000 beats applied at a basic cycle length of 1000 ms. The Euler method was implemented with a time step of 0.001 ms and lead concentrations from 0 to 1000 nM. The ionic currents and action potential duration (APD), at a 90% repolarization (APD_{90}), were measured on the 1000th beat.

3 Results and Discussion

3.1 Characterization and Real Particle Size Calculation

The thermogravimetric analysis (TGA) and differential thermal analysis (DTG) of the samples are shown in Fig. 1. An initial weight loss of 57.64% can be identified between 100 and 440 °C (maximum peak at 242 °C). This weight loss corresponds to humidity and water adsorbed by the material, and it could also be related to the loss of volatile material, since the volatilization of organic compounds is evident at temperatures below 462 °C. A second thermal event between 462 and 500 °C represents a weight loss of 4.39%, which is associated with elemental carbon. The remaining weight after the analysis (37.97%) is related to inorganic residues mainly composed of metal oxides and filter residues.

Volatile matter has been typically emitted by several anthropogenic sources, such as the degradation of fossil fuels and lubricant oil from motor vehicles (Chien et al. 2009; Santos et al. 2017a). In turn, elemental carbon is emitted during the incomplete combustion of fossil fuels and biomass burning. However, in order to consider elemental carbon to be an indicator of PM produced by burning fossil fuels in the environment, the geographical space where the sample was taken should be taken into account (Schauer 2003). The University of Medellín is located in a residential area, where the possibility of burning biomass is minimal. For that reason, the elemental

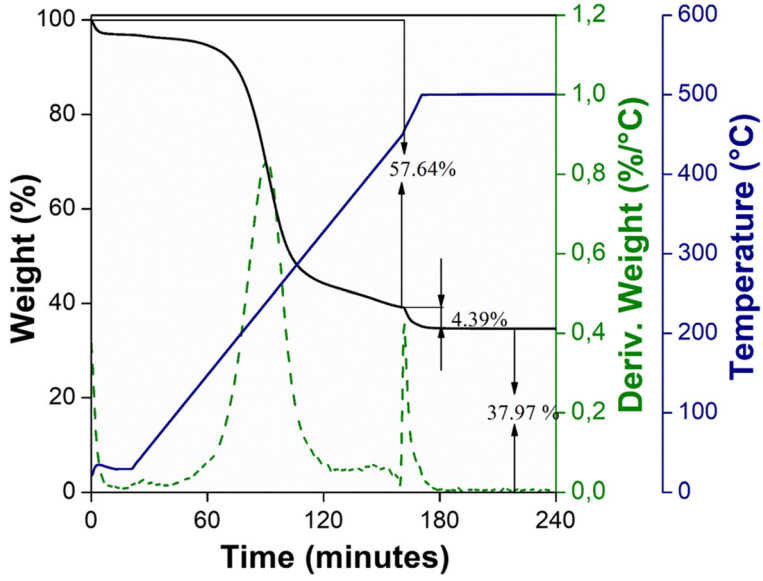

Fig. 1 Thermogravimetric analysis (TGA) and differential thermal analysis (DTG) of particulate matter

carbon found in the samples collected there could be mainly attributed to vehicles.

Figure 2 shows the FTIR spectra of the PM, which were obtained in order to evaluate the vibration of the functional groups in the sample. The absorption peak at around 3412 cm^{-1} is associated with O-H stretching vibration (Gipson et al. 2015). The band from 2845 cm^{-1} to 2919 cm^{-1} corresponds to symmetric and asymmetric C-H stretching vibration of the mainly aliphatic CH_2 group (Anil et al. 2014). The stretching vibration of C=O appears between 1375 cm^{-1} and 1630 cm^{-1} (Ge et al. 2017). The peak at 1450 cm^{-1} may be attributed to CO_2 vibrations (Roy et al. 2015). The bands between 1080 cm^{-1} and 1130 cm^{-1} are due to C-O stretching vibrations (Kharazmi et al. 2015; Hamzah et al. 2018). Finally, the vibrations at around 1870 cm^{-1}, 726 cm^{-1}, and 811 cm^{-1} can be associated with Si-O, Si-H, and Si-O-Si, respectively.

The TGA analysis revealed weight losses related to humidity, unburned fuel, motor oil, and silicon fibers. These results are in agreement with the FTIR due to the presence of the OH vibration of water and carbonyl (C=O), CO, and aliphatic C-H groups, which are associated with unburned fuel and motor oil (Correa and Arbilla 2008; Angelovi et al. 2013; Kupareva et al. 2013; Popovicheva et al. 2015). The primary source of anthropogenic CO_2 is the combustion of fossil fuels and industrial activities (Goldstein et al. 2017); in particular, fuels are a complex mixture of chemicals, several of them toxic and carcinogenic, which could have a strong impact on human health (Madanhire and Mbohwa 2016). For instance, the exposure to lubricating oils can cause skin and eye irritation (Hilpert et al. 2015).

As mentioned above, different particle sizes pose a problem for PM classification and have diverse effects on human health. However, studies into PM do not usually report particle size, which is assumed based on the type of collector used in air monitoring stations. Figure 3(a) and (b) show representative SEM micrographs of the PM in the filter before the extraction process. Figure 3(c) is a micrograph of the material obtained after the extraction process, and Fig. 3(d) presents a clean quartz microfiber filter before use for comparison**.** Particles attached to the fibers can be observed in micrographs (a) and (b). In all the cases, semispherical particles with a smooth surface morphology were found, in addition to a high particle size distribution. Micrograph (c) reveals the presence of

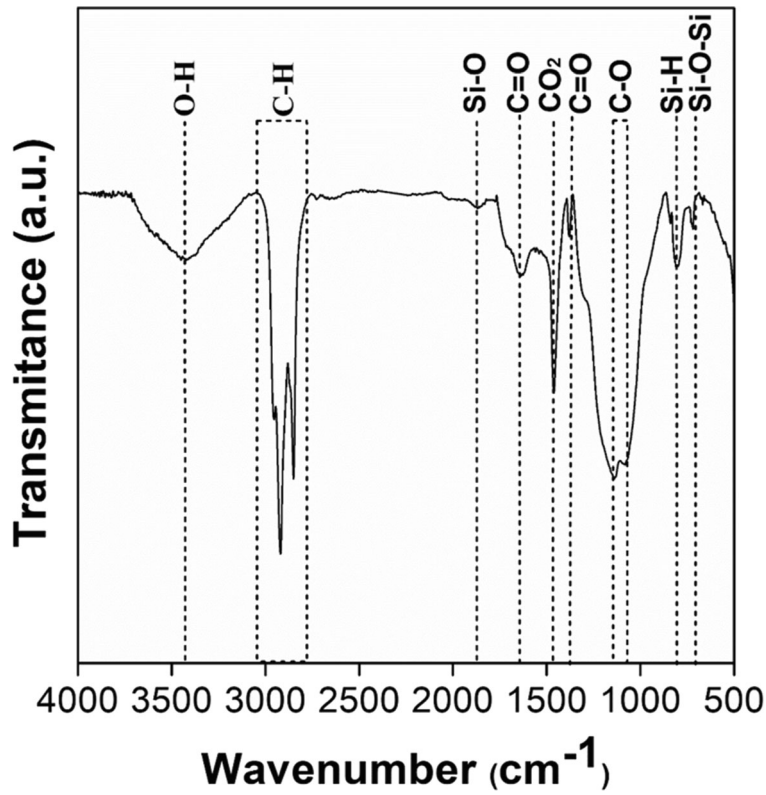

Fig. 2 Fourier-transform infrared spectroscopy (FTIR) of PM after the washing process

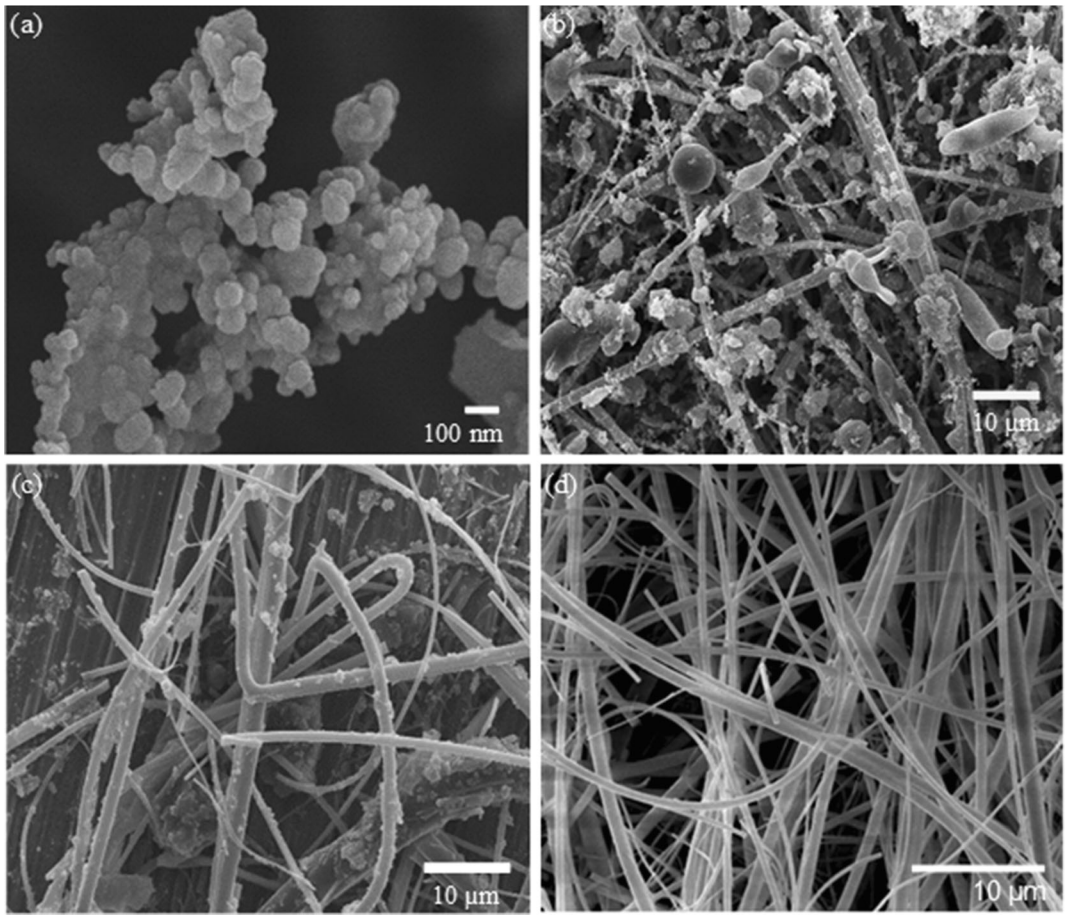

Fig. 3 Scanning electron micrographs (SEM) of quartz microfiber filters: (**a** and **b**) before the PM washing process at high and low magnifications, respectively; (c) filter after such washing process; and (**d**) brand new filter

particles and multiple detached filter fibers after the washing process. Fiber remnants are unavoidable after the washing process, and additional filtering is necessary to remove them.

The average diameter of the particles in the SEM images was measured by ImageJ software. The particle size distribution was first divided into three groups, and the results are shown in three histograms (Fig. 4). Figure 4(a) and (b) presents the size distributions of ultrafine (< 0.1 μm) and fine (between 0.1 and 2.5 μm) particles in the sample, respectively. Both fine and ultrafine PM are considered $PM_{2.5}$. In turn, the size distribution of coarse particles (> 2.5 μm) is detailed in Fig. 4(c). The ultrafine particles exhibit an average size of 0.056 μm, while the average sizes of fine and coarse particles are 1.84 and 4.5 μm, respectively.

Considering that the equipment used in this study was a certified PM_{10} collector, two important findings can be highlighted form these results. On the one hand, there is a big proportion of particles under 0.1 μm (ultrafine), which are typically considered in the $PM_{2.5}$ group and have been proven to be much more harmful than their microscopic counterparts. In that sense, this type of material deserves special attention in particulate material characterization (Li et al. 2018). On the other hand, the mean size of the coarse particles was found to be 4.5 μm. All the studies in the literature and the monitoring station reports include such particles in the PM_{10} group (10 μm) without any further discussion on particle size or its different effects.

Some aggregates were observed in the images. They are usually composed of primary particles with a uniform diameter (between 4 nm and 55 nm) and are formed by van der Waals, electrostatic, and surface adhesive forces (Yang et al. 2016). It has been reported that such particles are mainly emitted by road transport,

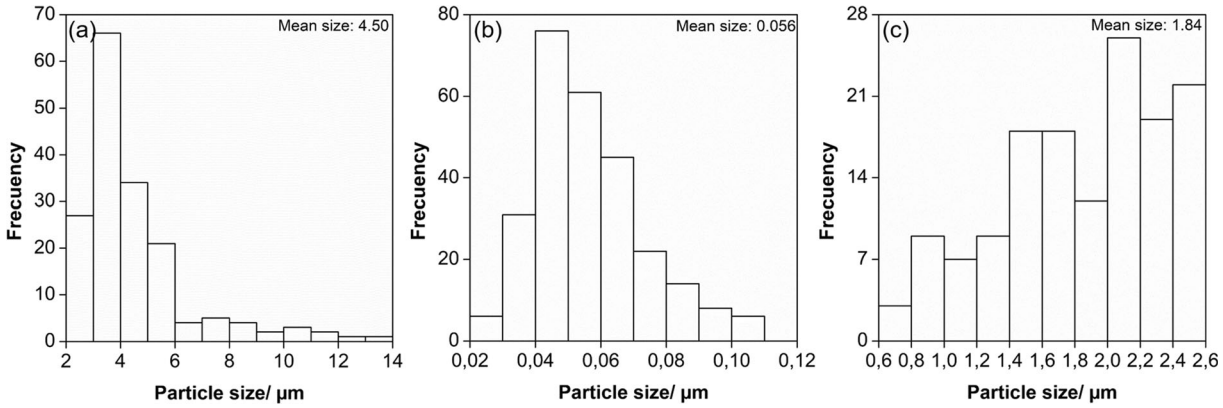

Fig. 4 Histogram of size distributions of the (**a**) ultrafine, (**b**) fine, and (**c**) coarse particles in the PM sample

industrial processes, and stationary combustion (Liati et al. 2016).

In the histogram in Fig. 4, the particle sizes range between 0.02 and 14 μm. This indicates a higher presence of ultrafine and fine particles in the collected PM, which is associated with serious problems for human health (Bai et al. 2018; Billet et al. 2018; Rajput et al. 2019). As mentioned before, such particles have their origin in natural sources (volcanic emissions and wildfires) as well as anthropogenic ones (traffic, electricity plants, and agriculture) (Gauterin et al. 2017). In general, PM whose diameter exceeds 10 μm can be largely filtered out by the nose and the upper airways. Nevertheless, fine and ultrafine particles can deposit into the lungs and the respiratory system, and they cannot be easily eliminated (Xia et al. 2018).

The lungs are the first target of air pollution. PM is associated with asthma, respiratory infections, and chronic obstructive pulmonary disease (Anderson et al. 2012). In addition, due to their size, ultrafine particles can move from the lungs into the blood stream and negatively impact the heart function, brain, and blood vessels with fatal consequences (Martinelli et al. 2013). Furthermore, ultrafine PM can directly enter the cells. Marchini et al. (Marchini et al. 2013) reported an impaired mitochondrial function in heart tissue samples after exposure to airborne PM, which was associated with reduced cardiac contractility.

Although particle size is a very important parameter in PM characterization, chemical composition is also necessary to identify the possible effects and different sources of PM. The chemical composition of the PM collected in this study was obtained by Energy Dispersive X-ray Spectroscopy (EDS) through a statistical analysis of different zones in the samples. Figure 5 shows an EDS spectrum of the PM with the presence

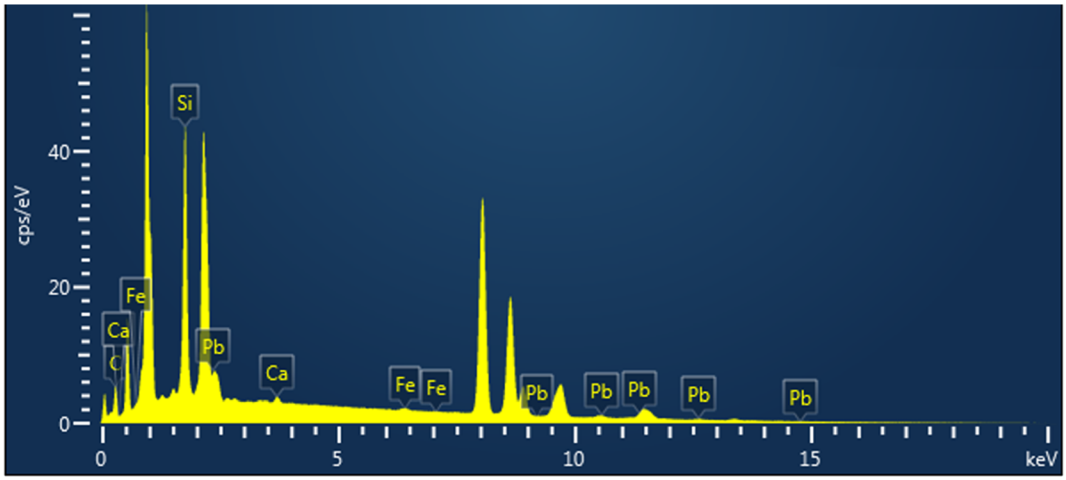

Fig. 5 Representative energy dispersive spectrum (EDS) of the particulate matter

of elements such as carbon (C), silicon (Si), iron (Fe), calcium (Ca), and lead (Pb).

Figure 6 shows the element distribution map obtained from the PM sample. Such EDS mapping identified the same elements found in the EDS spectrum (carbon, silicon, iron, calcium, titanium, aluminum, and lead). More specifically, the silicon (Si) is associated with the quartz microfiber filter used for sampling and detached during washing; for that reason, it was not analyzed in this study.

Table 1 shows the weight percentage (wt%) of the elements found in the sample by EDS analysis. To obtain these results, at least 20 samples were analyzed and weighted. Importantly, the high standard deviation they present is associated with the high heterogeneity of the samples and the reduced volume of analysis in the EDS.

Carbon, silicon, and lead are the most abundant elements in the analysis, and all of them have harmful effects on human health. However, as mentioned before, the presence of silicon is related to filter residues, which could not be separated from the PM. Carbon is associated with vehicular, industrial, and domestic emissions (Jandacka et al. 2017); in turn, the combustion of fossil fuels has been established as the main source of lead (Crilley et al. 2017). Lead is also one of the most widely investigated metals due to its negative influence on the environment and human health. According to the United States Environmental Protection Agency (EPA), lead is one of the most dangerous air pollutants, affecting multiple human body systems (U.S. EPA. 2013).

Colombian regulations allow the commercialization of fourth generation engines. Nevertheless, such technology has been available since 2005, which suggests that the vehicles in this country are considerably outdated in terms of the technological level of the engines and could explain the high levels of pollutant emissions (Martinez-Angel 2018). At the local level, two-stroke motorcycles, trucks, and dump trucks are the mobile sources that produce most emissions of particulate matter in Medellín, but fixed sources also make an important contribution to environmental pollution there (Área Metropolitana Valle de Aburrá 2018). According to a different study, in 2015, Medellín was home to 188 companies, which emitted 144.9 tons of PM_{10}, 30 tons of 2.5 ppm, and 56 kg of lead (Área Metropolitana Valle de Aburrá 2017). The presence of Ca, Al, and Ti in this study could be associated with the operation of a quarry located 145 m form the sampling point. It is well known that civil construction and

Table 1 Weight percentage (wt%) of the elements found in the sample by EDS

Element	Weight percentage (wt.%)			
	Mean	Deviation	Minimum	Maximum
Carbon	6.93	2.62	3.27	11.71
Silicon	5.31	3.39	1.99	10.43
Lead	2.72	1.74	1.76	6.18
Calcium	0.15	0.15	0.05	0.49
Iron	0.15	0.076	0.1	0.24
Titanium	0.96	0.3	0.89	1.47
Aluminum	1.13	0.92	0.48	1.79

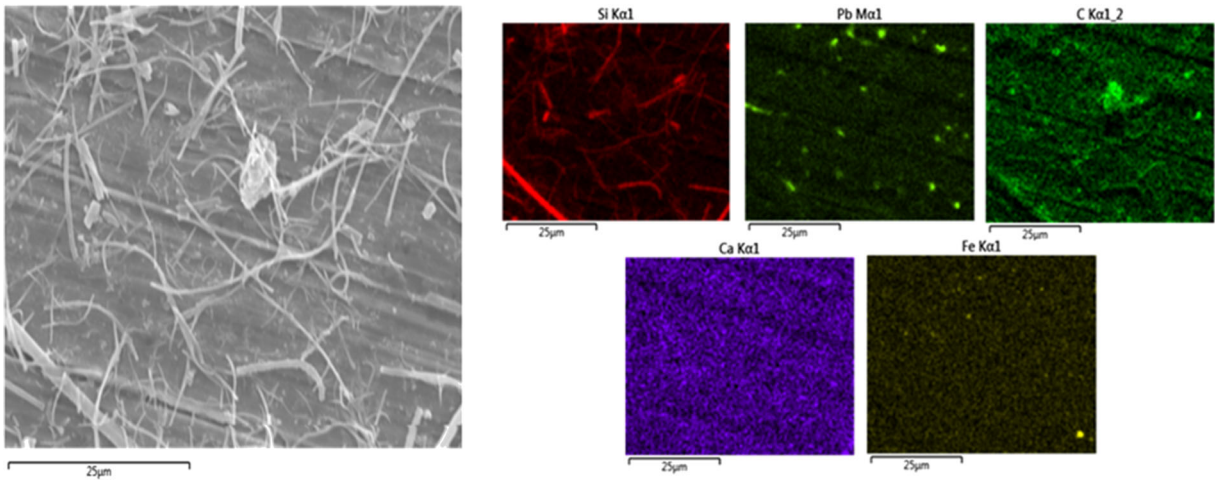

Fig. 6 Representative element distribution map of the particulate matter

quarries are significant contributors of such elements (Bluvshtein et al. 2011; Minguillón et al. 2013; Santos et al. 2017b). Moreover, Medellín has been ranked as the second city in Colombia with the largest number of square meters devoted to construction, which suggests an increase in cement consumption (DANE 2018). The presence of iron in the PM is caused by companies and vehicles (Jia et al. 2018). Although several authors have reported the presence of other heavy metals in PM, such as Cr, As, Cd, and Hg (Vimercati et al. 2017; Esposito et al. 2019), they were not found in this study. The absence of those elements in the atmosphere may be due to the fact that they come from industrial, agricultural, domestic, and technological sources that change from place to place.

Inductively coupled plasma-optical emission spectrometry (ICP-OES) was used in order to confirm the presence of lead in the sample, which was found at a concentration of 6940 nM. As mentioned before, lead is the most important toxic heavy element in the environment, since it causes serious problems to human health. Lead is a cumulative toxicant, and the severity of the symptoms it causes increases with exposure (World Health Organization 2018). Consequently, it remains a

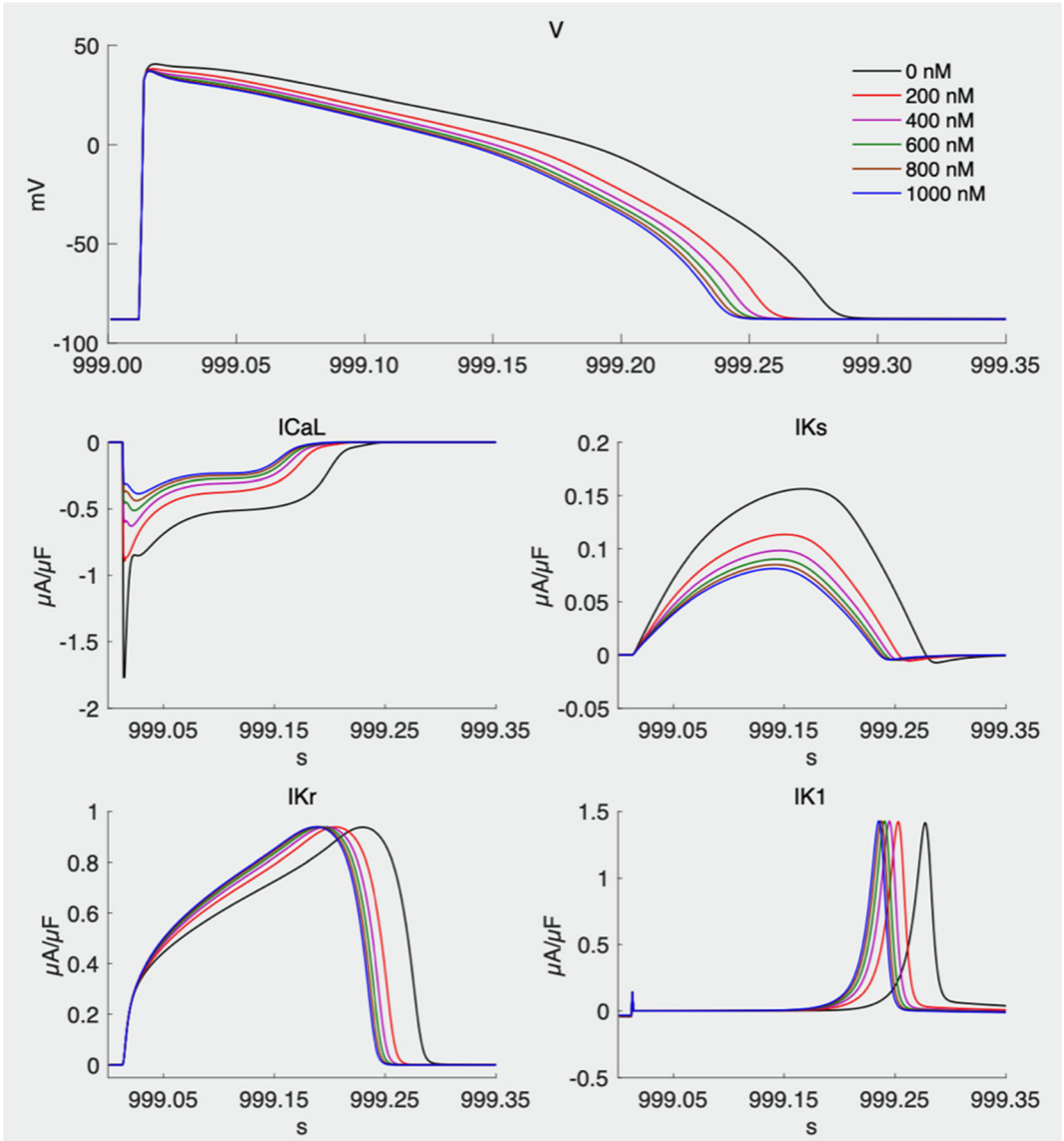

Fig. 7 Effect of lead at different concentrations on the action potential and I_{CaL}, I_{Ks}, I_{Kr} and I_{K1} currents

serious issue in both developed and developing countries (Tong et al. 2000; Tuakuila et al. 2013; World Health Organization 2019), where children are more vulnerable than adults to its effects (González et al. 2018). For those reasons and based on these results, we analyzed the effect of lead on the cardiac action potential.

3.2 Effect of Lead on Ventricular Action Potential

The results of the PM characterization showed high concentrations of C, Si, and Pb. Because carbonaceous materials have already been widely studied and Si is mostly related to the filter's material, lead was selected to investigate its effect on ventricular action potential by means of computer simulations. Figure 7 shows the effects of different lead concentrations on the main ionic currents and the ventricular action potential. Under control conditions (without lead), the maximum current peaks of I_{CaL} and the slowly activating potassium current (I_{Ks}) were −1.74 μA/μF and 0.15 μA/μF, respectively; the rapidly activating potassium current (I_{Kr}) and the inwardly rectifying potassium current (I_{K1}) had maximum peaks at 999.229 and 999.277 s, respectively; and the APD_{90} reached 266 ms. As the lead concentration was increased, a downregulation of I_{CaL} and I_{Ks} was observed, and the I_{Kr} and I_{K1} curves shifted to the left, which caused an APD shortening. When the highest lead concentration was applied (1000 nM), the I_{CaL} and I_{Ks} peaks showed values of −0.55 μA/μF and 0.07 μA/μF, indicating decreases of 68% and 53%, respectively; the I_{Kr} and I_{K1} curves shifted to the left by 46 ms and 48 ms (maximum peaks at 999.183 s and 999.229 s), respectively; and the APD_{90} reached 220 ms, which is a 17% decrease.

The results show that lead concentrations above 600 nM produce similar effects on APD shortening: 600, 800, and 1000 nM caused reductions of 15, 16, and 17% respectively. Therefore, it was not necessary to study of the value of lead found by ICP. The calcium channel block by lead has been reported in other cell types (Atchison 2003; Peng et al. 2002). In cardiac tissue, the L-type calcium channel block by lead was experimentally demonstrated by Bernal et al. (1997), whose study into the ventricular myocytes of rats showed that lead blocks the I_{CaL}, generating alterations in other ionic currents and an APD shortening. Such alterations can significantly reduce the theoretical limit of the path length required for the development or maintenance of reentries, which initiate and sustain cardiac arrhythmias (Antzelevitch and Burashnikov 2011). Reduced APD in human cardiac tissue is the most likely cause of the reentries underlying ventricular tachycardias (Ten Tusscher et al. 2009). Ferreira de Mattos et al. (2017) in isolated cardiomyocytes, tsA 201 cells, and isolated guinea pig hearts, reported that lead was cardiotoxic and reduced cardiac contractility, making the heart prone to arrhythmias. This was attributed, in part, to the effects of extracellular lead in blocking calcium currents through Cav1.2 channels.

4 Conclusions

PM_{10} collected in Medellín, Colombia, was physicochemically characterized in this study. Particle sizes between 0.056 and 4.5 μm were found, which indicates the presence of the most harmful particles for human health, according to the WHO, in that city. Nevertheless, the amount of this kind of PM is typically underestimated in all the collectors used for PM detection.

A great concentration of carbonaceous materials, which are related to the incomplete combustion of fuel and engine lubricant, was present in the sample. Additionally, metals such as Ca, Si, Pb, Ca, Fe, Ti, and Al were found in the PM and quantified; they are associated with a quarry near the sampling station, the burning of fossil fuels, and soil particles.

Lead, the most harmful heavy metal for human health identified in the sample, was further studied, and our results show it has a pro-arrhythmic effect that is reflected in a shortening of the APD. Computational studies may contribute to a better understanding of the mechanisms by which PM has unhealthy effects on cardiac tissue, promoting cardiac diseases such as arrhythmias.

Funding This work was funded by Ministerio de Ciencia, Tecnología e Innovación (MINCIENCIAS) in Colombia through grant No. 120677757994.

Compliance with Ethical Standards

Conflict of Interest The authors declare that they have no conflict of interest.

References

Al-Thani, H., Koç, M., & Isaifan, R. J. (2018). A review on the direct effect of particulate atmospheric pollution on materials and its mitigation for sustainable cities and societies. *Environmental Science and Pollution Research, 25*, 27839–27857. https://doi.org/10.1007/s11356-018-2952-8.

Anderson, J. O., Thundiyil, J. G., & Stolbach, A. (2012). Clearing the air : a review of the effects of particulate matter air pollution on human health. *Journal of Medical Toxicology, 8*, 166–175. https://doi.org/10.1007/s13181-011-0203-1.

Angelovi, M., Tká, Z., & Angelovi, M. (2013). Particulate emissions and biodiesel: a review. *Animal Science and Biotechnology, 46*, 192–198.

Anil, I., Golcuk, K., & Karaca, F. (2014). ATR-FTIR spectroscopic study of functional groups in aerosols: the contribution of a Saharan dust transport to urban atmosphere in Istanbul, Turkey. *Water, Air, and Soil Pollution, 225*, 3–14. https://doi.org/10.1007/s11270-014-1898-9.

Antzelevitch, C., & Burashnikov, A. (2011). Overview of basic mechanisms of cardiac arrhythmia. *Cardiac Electrophysiology Clinics, 3*, 23–45.

Área Metropolitana Valle de Aburrá (2017) *Inventario de emisiones atmosféricas del Valle de Aburrá, actualización 2015*. pp 1–48. https://www.metropol.gov.co/ambiental/calidad-del-aire/Documents/Inventario-de-emisiones/Inventario_FuentesM%C3%B3viles2016.pdf

Área Metropolitana Valle de Aburrá. (2018). *Actualización Inventario de Emisiones Atmosféricas del Valle de Aburrá - Año, 2016*, 1–62.

Arias-Valencia, R., Nolasco Bonmatí, A., Pereyra-Zamora, P., et al. (2010). Diseño y análisis comparativo de un inventario de indicadores de mortalidad evitable adaptado a las condiciones sanitarias de Colombia. *Revista Panamericana de Salud Pública, 26*, 385–397. https://doi.org/10.1590/s1020-49892009001100002.

Atchison, W. D. (2003). Effects of toxic environmental contaminants on voltage-gated calcium channel function: From past to present. *Journal of Bioenergetics and Biomembranes, 35*, 507–532. https://doi.org/10.1023/b:jobb.0000008023.11211.13.

Babick, F., Mielke, J., Wohlleben, W., et al. (2016). How reliably can a material be classified as a nanomaterial? Available particle-sizing techniques at work. *Journal of Nanoparticle Research, 18*, 1–40. https://doi.org/10.1007/s11051-016-3461-7.

Bai, X., Liu, Y., Wang, S., et al. (2018). Ultrafine particle libraries for exploring mechanisms of PM2.5-induced toxicity in human cells. *Ecotoxicology and Environmental Safety, 157*, 380–387. https://doi.org/10.1016/j.ecoenv.2018.03.095.

Bañeras, J., Ferreira-González, I., Marsal, J. R., et al. (2018). Short-term exposure to air pollutants increases the risk of ST elevation myocardial infarction and of infarct-related ventricular arrhythmias and mortality. *International Journal of Cardiology, 250*, 35–42. https://doi.org/10.1016/J.IJCARD.2017.10.004.

Bernal, J., Lee, J., Cribbs, L. L., & Perez-reyes, E. (1997). Full reversal of Pb++ block of L-type Ca++ channels requires treatment with heavy metal antidotes. *The Journal of Pharmacology and Experimental Therapeutics, 282*, 172–180.

Billet, S., Landkocz, Y., Martin, P. J., et al. (2018). Chemical characterization of fine and ultrafine PM, direct and indirect genotoxicity of PM and their organic extracts on pulmonary cells. *Journal of Environmental Sciences, 71*, 168–178. https://doi.org/10.1016/j.jes.2018.04.022.

Bluvshtein, N., Mahrer, Y., Sandler, A., & Rytwo, G. (2011). Evaluating the impact of a limestone quarry on suspended and accumulated dust. *Atmospheric Environment, 45*, 1732–1739. https://doi.org/10.1016/j.atmosenv.2010.12.055.

Bozkurt, Z. O., Gaga, E., Taşpınar, F., et al. (2018). Atmospheric ambient trace element concentrations of PM10 at urban and sub-urban sites: Source apportionment and health risk estimation. *Environmental Monitoring and Assessment, 190*, 168. https://doi.org/10.1007/s10661-018-6517-6.

Cavanagh, J.-A. E., Trought, K., Brown, L., & Duggan, S. (2009). Exploratory investigation of the chemical characteristics and relative toxicity of ambient air particulates from two New Zealand cities. *Science of the Total Environment, 407*, 5007–5018. https://doi.org/10.1016/J.SCITOTENV.2009.05.020.

Chien, Y., Lu, M., Chai, M., & Boreo, F. J. (2009). Characterization of biodiesel and biodiesel particulate matter by TG , TG - MS , and FTIR. *Energy and Fuels, 23*, 202–206.

Chin, M. T. (2015). Basic mechanisms for adverse cardiovascular events associated with air pollution. *Heart, 101*, 253–256. https://doi.org/10.1136/heartjnl-2014-306379.

Correa, S., & Arbilla, G. (2008). Carbonyl emissions in diesel and biodiesel exhaust. *Atmospheric Environment, 42*, 769–775. https://doi.org/10.1016/j.atmosenv.2007.09.073.

Crilley, L. R., Lucarelli, F., Bloss, W. J., et al. (2017). Source apportionment of fi ne and coarse particles at a roadside and urban background site in London during the 2012 summer ClearfLo. *Environmental Pollution, 220*, 766–778. https://doi.org/10.1016/j.envpol.2016.06.002.

Dallarosa, J. B., Teixeira, E. C., Pires, M., & Fachel, J. (2005). Study of the profile of polycyclic aromatic hydrocarbons in atmospheric particles (PM10) using multivariate methods. *Atmospheric Environment, 39*, 6587–6596. https://doi.org/10.1016/J.ATMOSENV.2005.07.034.

Davy, P. K., Ancelet, T., Trompetter, W. J., et al. (2012). Composition and source contributions of air particulate matter pollution in a New Zealand suburban town. *Atmospheric Pollution Research, 3*, 143–147. https://doi.org/10.5094/APR.2012.014.

De Kok, T. M., Hogervorst, J. G., Briedé, J. J., et al. (2005). Genotoxicity and physicochemical characteristics of traffic-related ambient particulate matter. *Environmental and Molecular Mutagenesis, 46*, 71–80. https://doi.org/10.1002/em.20133.

Departamento Administrativo Nacional de Estadística - DANE. (2018). *Boletín técnico censo edificaciones (CEED)* (pp. 1–40). Censo: Bogotá D.C.CO. Sec.

Di Novi, C. (2013). The indirect effect of fine particulate matter on health through individuals' life-style. *The Journal of Socio-Economics, 44*, 27–36. https://doi.org/10.1016/j.socec.2013.02.002.

Dickerson, A. S., Benson, A. F., Buckley, B., & Chan, E. A. W. (2016). Concentrations of individual fine particulate matter components in the USA around July 4th. *Air Quality,*

Atmosphere and Health, 10, 349–358. https://doi.org/10.1007/s11869-016-0433-0.

Dutta, S., Chang, K. C., Colatsky, T., et al. (2017). Optimization of an in silico cardiac cell model for proarrhythmia risk assessment. *Frontiers in Physiology, 8*, 1–15. https://doi.org/10.3389/fphys.2017.00616.

Esposito, F., Memoli, V., Di Natale, G., et al. (2019). Quercus ilex L. leaves as filters of air cd, Cr, cu, Ni and Pb. *Chemosphere, 218*, 340–346. https://doi.org/10.1016/j.chemosphere.2018.11.133.

Ferreira de Mattos, G., Costa, C., Savio, F., et al. (2017). Lead poisoning: acute exposure of the heart to lead ions promotes changes in cardiac function and Cav1.2 ion channels. *Biophysical Reviews, 9*, 807–825. https://doi.org/10.1007/s12551-017-0303-5.

Gauterin, F., Dörnhöfer, J., Foitzik, M.-J., et al. (2017). Investigation of ultra fine particulate matter emission of rubber tires. *Wear, 394–395*, 87–95. https://doi.org/10.1016/j.wear.2017.09.023.

Ge, S., Liu, Z., Furuta, Y., & Peng, W. (2017). Characteristics of activated carbon remove sulfur particles against smog. *Saudi Journal of Biological Sciences, 24*, 1370–1374. https://doi.org/10.1016/j.sjbs.2016.12.016.

Genga, A., Siciliano, T., Siciliano, M., et al. (2018). Individual particle SEM-EDS analysis of atmospheric aerosols in rural, urban, and industrial sites of Central Italy. *Environmental Monitoring and Assessment, 190*, 456. https://doi.org/10.1007/s10661-018-6826-9.

Gipson, K., Stevens, K., Brown, P., & Ballato, J. (2015). Infrared spectroscopic characterization of Photoluminescent polymer Nanocomposites. *Journal of Spectroscopy, 2015*, 1–9.

Goldstein, A. O., Gans, S. P., Ripley-mof, C., et al. (2017). Use of expired air carbon monoxide testing in clinical tobacco treatment settings. *Chest, 153*, 554–562. https://doi.org/10.1016/j.chest.2017.11.002.

Gomez M, Dawidowski L, Posada E, et al. (2011) Chemical composition of PM2.5 in three zones of the Aburrá Valley, Medellin, Colombia. In: Proceedings of the Air and Waste Management Association's Annual Conference and Exhibition, AWMA. pp 2534–2545.

González, L. T., Longoria-Rodríguez, F. E., Sánchez-Domínguez, M., et al. (2018). Seasonal variation and chemical composition of particulate matter: a study by XPS, ICP-AES and sequential microanalysis using Raman with SEM/EDS. *Journal of Environmental Sciences, 74*, 32–49. https://doi.org/10.1016/j.jes.2018.02.002.

Hamzah M, MKhenfouch M, Rjeb A, et al. (2018) Surface chemistry changes and microstructure evaluation of low density nanocluster polyethylene under natural weathering : a spectroscopic investigation. In: Journal of physics: Conference series. Pp 1–15.

Hilpert, M., Mora, B. A., Ni, J., et al. (2015). Hydrocarbon release during fuel storage and transfer at gas stations: environmental and health effects. *Current Environmental Health Reports, 2*, 412–422. https://doi.org/10.1007/s40572-015-0074-8.

Huang, K. L., Liu, S. Y., Chou, C. C. K., et al. (2017). The effect of size-segregated ambient particulate matter on Th1/Th2-like immune responses in mice. *PLoS One, 12*, 1–16. https://doi.org/10.1371/journal.pone.0173158.

Jandacka, D., Durcanska, D., & Bujdos, M. (2017). The contribution of road traffic to particulate matter and metals in air pollution in the vicinity of an urban road. *Transportation Research Part D: Transport and Environment, 50*, 397–408. https://doi.org/10.1016/j.trd.2016.11.024.

Jia, J., Cheng, S., Yao, S., et al. (2018). Emission characteristics and chemical components of size-segregated particulate matter in iron and steel industry. *Atmospheric Environment, 182*, 115–127. https://doi.org/10.1016/j.atmosenv.2018.03.051.

Kharazmi, A., Faraji, N., Hussin, R. M., et al. (2015). Structural, optical, opto-thermal and thermal properties of ZnS–PVA nanofluids synthesized through a radiolytic approach. *Beilstein Journal of Nanotechnology, 6*, 529–536. https://doi.org/10.3762/bjnano.6.55.

Kholdebarin, A., Biati, A., Moattar, F., & Shariat, S. M. (2015). Outdoor PM_{10} source apportionment in metropolitan cities—A case study. *Environmental Monitoring and Assessment, 187*, 49. https://doi.org/10.1007/s10661-015-4294-z.

Kupareva, A., Mäki-Arvela, P., Grénman, H., et al. (2013). Chemical characterization of lube oils. *Energy and Fuels, 27*, 27–34. https://doi.org/10.1021/ef3016816.

Li, Q., Zhu, Z., Hu, R., et al. (2018). Fine particulate matter (PM2.5): The culprit for chronic lung diseases in China. *Chronic Diseases and Translational Medicine, 4*, 176–186. https://doi.org/10.1016/j.cdtm.2018.07.002.

Liati, A., Schreiber, D., Dimopoulos, P., et al. (2016). Electron microscopic characterization of soot particulate matter emitted by modern direct injection gasoline engines. *Combustion and Flame, 166*, 307–315. https://doi.org/10.1016/j.combustflame.2016.01.031.

Lim, Y.-H., Bae, H.-J., Yi, S., et al. (2017). Vascular and cardiac autonomic function and PM2.5 constituents among the elderly: A longitudinal study. *Science of the Total Environment, 607–608*, 847–854. https://doi.org/10.1016/j.scitotenv.2017.07.077.

López, R. A., Luis, J., Arango, M., et al. (2017). *Informe de calidad de vida de Medellín, 2016* (pp. 1–201). Medellín: Pregón S.A.S.

Lu, J., Ma, L., Cheng, C., et al. (2019). Real time analysis of lead-containing atmospheric particles in Guangzhou during wintertime using single particle aerosol mass spectrometry. *Ecotoxicology and Environmental Safety, 168*, 53–63. https://doi.org/10.1016/j.ecoenv.2018.10.006.

Lustbeg, M., & Silbergeld, E. (2015). Blood Lead levels and mortality. *American Medical Association, 162*, 2443–2449.

Madanhire I, Mbohwa C (2016) Mitigating environmental impact of petroleum lubricants. In: *Mitigating Environmental Impact of Petroleum Lubricant*s. pp. 1–239.

Marchini, T., Magnani, N., Annunzio, V. D., et al. (2013). Impaired cardiac mitochondrial function and contractile reserve following an acute exposure to environmental particulate matter. *Biochimica et Biophysica Acta, 1830*, 2545–2552. https://doi.org/10.1016/j.bbagen.2012.11.012.

Martinelli, N., Olivieri, O., & Girelli, D. (2013). Air particulate matter and cardiovascular disease : A narrative review. *European Journal of Internal Medicine, 24*, 295–302. https://doi.org/10.1016/j.ejim.2013.04.001.

Martinez-Angel, J. D. (2018). Movilidad motorizada, impacto ambiental, alternativas y perspectivas futuras: consideraciones para el Área Metropolitana del Valle de Aburrá. *Revista Salud Pública, 20*, 126–131. https://doi.org/10.15446/rsap.v20n1.57038.

Masih, A., Saini, R., Singhvi, R., & Taneja, A. (2010). Concentrations, sources, and exposure profiles of polycyclic aromatic hydrocarbons (PAHs) in particulate matter (PM10) in the north central part of India. *Environmental Monitoring and Assessment, 163*, 421–431. https://doi.org/10.1007/s10661-009-0846-4.

Mazzoli, A., & Favoni, O. (2012). Particle size, size distribution and morphological evaluation of airborne dust particles of diverse woods by scanning electron microscopy and image processing program. *Powder Technology, 225*, 65–71. https://doi.org/10.1016/j.powtec.2012.03.033.

Menke, A., Muntner, P., Batuman, V., et al. (2006). Blood lead below 0.48 umol/L (10 μg/dL) and mortality among US adults. *Epidemiology, 114*, 1388–1394. https://doi.org/10.1161/CIRCULATIONAHA.106.628321.

Minguillón, M. C., Monfort, E., Escrig, A., et al. (2013). Air quality comparison between two European ceramic tile clusters. *Atmospheric Environment, 74*, 311–319. https://doi.org/10.1016/j.atmosenv.2013.04.010.

Mirowsky, J., Hickey, C., Horton, L., et al. (2014). The effect of particle size, location and season on the toxicity of urban and rural particulate matter. *Beilstein Journal of Nanotechnology, 5*, 1590–1602. https://doi.org/10.3109/08958378.2013.846443.

Moreira-Lopez, T. C., Oliveira, R. C., Amato, L. F., et al. (2016). Intra-urban biomonitoring : Source apportionment using tree barks to identify air pollution sources. *Environment International, 91*, 271–275. https://doi.org/10.1016/j.envint.2016.03.005.

Müller, K., Spindler, G., Herrmann, H., et al. (2017). Assessment of trace metal levels in size-resolved particulate matter in the area of Leipzig. *Atmospheric Environment, 176*, 60–70. https://doi.org/10.1016/j.atmosenv.2017.12.024.

Mustafi, N. N., Raine, R. R., & James, B. (2010). Characterization of exhaust particulates from a dual fuel engine by TGA , XPS , and Raman Techniques. *Aerosol Science and Technology, 44*, 954–963. https://doi.org/10.1080/02786826.2010.503668.

Obot, C. J., Morandi, M. T., Beebe, T. P., et al. (2002). Surface components of airborne particulate matter induce macrophage apoptosis through scavenger receptors. *Toxicology and Applied Pharmacology, 184*, 98–106. https://doi.org/10.1016/S0041-008X(02)99493-7.

Peng, S., Hajela, R. K., & Atchison, W. D. (2002). Characteristics of block by Pb2+ of function of human neuronal L-, N-, and R-type Ca2+ channels transiently expressed in human embryonic kidney 293 cells. *Molecular Pharmacology, 62*, 1418–1430. https://doi.org/10.1124/mol.62.6.1418.

Perrino, C., Tofful, L., & Canepari, S. (2015). Chemical characterization of indoor and outdoor fine particulate matter in an occupied apartment in Rome, Italy. *Indoor Air, 26*, 558–570. https://doi.org/10.1111/ina.12235.

Popovicheva, O. B., Kireeva, E. D., Shonija, N. K., et al. (2015). FTIR analysis of surface functionalities on particulate matter produced by off-road diesel engines operating on diesel and biofuel. *Environmental Science and Pollution Research, 22*, 4534–4544. https://doi.org/10.1007/s11356-014-3688-8.

Rajput, P., Izhar, S., & Gupta, T. (2019). Deposition modeling of ambient aerosols in human respiratory system: Health implication of fine particles penetration into pulmonary region. *Atmospheric Pollution Research, 10*, 334–343. https://doi.org/10.1016/j.apr.2018.08.013.

Roper, C., Chubb, L. G., Cambal, L., et al. (2015). Characterization of ambient and extracted $PM_{2.5}$ collected on filters for toxicology applications. *Inhalation Toxicology, 27*, 673–681. https://doi.org/10.3109/08958378.2015.1092185.

Roy, D., Gautam, S., Singh, P., et al. (2015). Carbonaceous species and physicochemical characteristics of PM10 in coal mine fire area — A case study. *Air Quality, Atmosphere and Health, 9*, 429–437. https://doi.org/10.1007/s11869-015-0355-2.

Santos, J. C. O., Santos, I. M. G., & Souza, A. G. (2017a). Thermal degradation of synthetic lubricating oils : Part III – TG and DSC studies. *Petroleum Science and Technology, 35*, 540–546. https://doi.org/10.1080/10916466.2016.1269127.

Santos, J. M., Reis Jr., C. N., et al. (2017b). Source apportionment of settleable particles in an impacted urban and industrialized region in Brazil. *Environmental Science and Pollution Research, 24*, 22026–22039. https://doi.org/10.1007/s11356-017-9677-y.

Schauer, J. J. (2003). Evaluation of elemental carbon as a marker for diesel particulate matter. *Exposure Analysis and Environmental Epidemiology, 13*, 443–453. https://doi.org/10.1038/sj.jea.7500298.

Škarek, M., Janošek, J., Čupr, P., et al. (2007). Evaluation of genotoxic and non-genotoxic effects of organic air pollution using in vitro bioassays. *Environment International, 33*, 859–866. https://doi.org/10.1016/j.envint.2007.04.001.

Ten Tusscher, K. H. W. J., Mourad, A., Nash, M. P., et al. (2009). Organization of ventricular fibrillation in the human heart: Experiments and models. *Experimental Physiology, 94*, 553–562. https://doi.org/10.1113/expphysiol.2008.044065.

Tong, S., von Schirnding, Y. E., & Prapamontol, T. (2000). Environmental lead exposure: a public health problem of global dimensions. *Bulletin of the World Health Organization, 78*, 1068–1077.

Tuakuila, J., Lison, D., Mbuyi, F., et al. (2013). Elevated blood lead levels and sources of exposure in the population of Kinshasa, the capital of the Democratic Republic of Congo. *Journal of Exposure Science & Environmental Epidemiology, 23*, 81–87. https://doi.org/10.1038/jes.2012.49.

U.S. EPA. (1999). *Compendium of methods for determination of inorganic compounds in ambient air*. Washington, DC: Cincinnati U.S. Environmental Protection Agency EPA/625/R-96/010a.

U.S. EPA. (2013). *Integrated science assessment (ISA) for Lead (final report, Jul 2013)*. Washington, DC: U.S. Environmental Protection Agency EPA/600/R-10/075F.

U.S. EPA. (2016). *Revisions to test methods, performance specifications, and testing regulations for air emission sources*. Washington, DC: U.S. Environmental Protection Agency 81 FR 59799.

U.S. EPA. (2018) Health and environmental effects of particulate matter (PM). U.S. Environmental Protection Agency. https://www.epa.gov/pm-pollution/health-and-environmental-effects-particulate-matter-pm. Accessed 30 May 2018.

Vimercati, L., Gatti, M. F., Gagliardi, T., et al. (2017). Environmental exposure to arsenic and chromium in an

industrial area. *Environmental Science and Pollution Research, 24*, 11528–11535. https://doi.org/10.1007/s11356-017-8827-6.

Wang, M., Kai, K., Sugimoto, N., & Enkhmaa, S. (2018). Meteorological factors affecting winter particulate air pollution in Ulaanbaatar from 2008 to 2016. *Asian Journal of Atmospheric Environment, 12*, 244–254. https://doi.org/10.5572/ajae.2018.12.3.244.

Wani, A. L., Ara, A., & Usmani, J. A. (2015). Lead toxicity: a review. *Interdisciplinary Toxicology, 8*, 55. https://doi.org/10.1515/INTOX-2015-0009.

World Health Organization (2018) Lead poisoning and health. https://www.who.int/news-room/fact-sheets/detail/lead-poisoning-and-health. Accessed 23 Aug 2018.

World Health Organization (2019) Ambient air pollution - a major threat to health and climate. https://www.who.int/airpollution/en/. Accessed 24 Aug 2019.

Wu, W., & Zhang, Y. (2018). Effects of particulate matter (PM2.5) and associated acidity on ecosystem functioning: response of leaf litter breakdown. *Environmental Science and Pollution Research, 25*, 30720–30727. https://doi.org/10.1007/s11356-018-2922-1.

Xia, T., Zhu, Y., Mu, L., et al. (2018). Pulmonary diseases induced by ambient ultrafine and engineered nanoparticles in twenty-first century. *National Science Review, 3*, 416–429. https://doi.org/10.1093/nsr/nww064.

Xing, Y. F., Xu, Y. H., Shi, M. H., & Lian, Y. X. (2016). The impact of PM2.5 on the human respiratory system. *Journal of Thoracic Disease, 8*, 69–74. https://doi.org/10.3978/j.issn.2072-1439.2016.01.19.

Yang, H., Li, X., Wang, Y., et al. (2016). Experimental investigation into the oxidation reactivity and nanostructure of particulate matter from diesel engine fuelled with diesel/polyoxymethylene dimethyl ethers blends. *Scientific Reports, 6*, 1–10. https://doi.org/10.1038/srep37611.